



Structural relaxation and quasi-elastic light scattering in glass: Approach by ferroelectric and ion-conducting phases

Yoshihiro Takahashi¹, Kensaku Nakamura¹, Minoru Osada² & Takumi Fujiwara¹

¹Department of Applied Physics, Tohoku University, 6-6-05 Aoba, Aoba-ku, Sendai 980-8579, Japan, ²International Center for Materials Nanoarchitectonics, National Institute for Materials Science, 1-1 Namiki, Tsukuba, Ibaraki 305-0044, Japan.

SUBJECT AREAS:

NANOSCIENCE AND
TECHNOLOGY

PHYSICAL CHEMISTRY

MATERIALS SCIENCE

CONDENSED-MATTER PHYSICS

Received

15 August 2012

Accepted

17 September 2012

Published

8 October 2012

Correspondence and requests for materials should be addressed to Y.T. (takahashi@laser.apph.tohoku.ac.jp)

Inelastic light scattering has been utilized for examining the structure of glass and its relaxation. However, the quasi-elastic-light-scattering (QLS) phenomenon has not been addressed in much detail. In this study, we observed pronounced QLS-intensity variations in two temperature domains—supercooled liquid (SCL) state (α -relaxation regime) and below the glass-transition temperature (β -relaxation regime)—in niobium-oxide (Nb_2O_5)-rich glass. These variations may be interpreted on the basis of the concept of ferroelectric and ion-conducting phases. It was suggested that the observed QLS originates as a result of the polarization fluctuation of NbO_6 units, which is due to the dynamics of the nanometric phase separation in the SCL phase (α -regime), and the fluctuation due to the migration/hopping of conductible ions that are localized in the vicinity of the NbO_6 units (β -regime).

Structural relaxation in glass and its subsequent ordering (i.e. crystallization) have been studied for a long time because these issues are important from scientific and engineering perspectives^{1–4}. Since a typical glass substance, niobium oxide (Nb_2O_5), plays a dual role of a network former and modifier (NM) in a glass-forming system (i.e. intermediate oxide), relaxation and ordering are closely related to the dynamics of the coordinated Nb units in the glass structure. On the other hand, since Nb-based ferroelectrics possess excellent properties because of the off-centred high polarizable NbO_6 unit, nanostructured glass ceramics (GC) with Nb ferroelectrics have been fabricated using Nb_2O_5 -rich glass as a precursor, with the aim of obtaining sophisticated dielectric/photonics materials^{5,6}. However, only the crystallized functional phase and its morphology, which are responsible for physical properties, have been addressed, and not much attention has been paid to the behaviour of the Nb units during the relaxation/crystallization process.

To examine the dynamics of relaxation and ordering, Takahashi et al. performed in situ observations of the Boson peak, which universally appears in low-frequency regions of amorphous matter. They observed that structural relaxation in the NM/intermediate cohesive region on a nanometric scale (~ 1 – 2 nm) triggers crystal nucleation^{7,8}. On the other hand, a scattering phenomenon, which appears at frequencies lower than the Boson-peak frequency, i.e. quasi-elastic light scattering (QLS) has not been addressed in much detail because it is difficult to embody its origin. Therefore, to clarify this issue, we conducted in situ spectroscopic measurements using Nb_2O_5 -rich (phosphoniobate) glass showing the nanostructuring of Nb ferroelectrics and attempted to interpret the origin of the QLS phenomenon in glassy matter, in addition with the Boson peak and Raman scattering results. We employed the Nb_2O_5 -rich glass as a test sample because three-dimensional (3D) interlinked NbO_6 units are present in the network structure, leading us to anticipate the application of QLS studies for Nb-based ferroelectrics to the Nb_2O_5 -rich glass, which have a similar framework.

Results

In situ observation of low-frequency light scattering. Fig. 1 shows the observation results of inelastic light scattering from the test sample, i.e. $0.67(2\text{BaO}-0.5\text{Na}_2\text{O})-1\text{P}_2\text{O}_5-2.5\text{Nb}_2\text{O}_5$ glass⁹, in the low-frequency region during heating. We observed a broad band, which is the so-called ‘Boson peak’, around ~ 64 cm^{-1} at room temperature (RT) [Fig. 1(a)]. After increasing the temperature, the frequency of the Boson peak (ω_{BP}) slightly decreased, while its full-width at half-maximum (FWHM) slightly increased over the temperature range of RT– 700°C (hereafter, this range is called ‘domain I’) [Fig. 1(b)]. In addition, for the range of 700 – 800°C (domain II), the ω_{BP} and FWHM began to decrease and broaden, respectively, and the Boson peak eventually disappeared/overdamped above 800°C (domain III), resulting in a structureless spectra. Furthermore, we observed that the

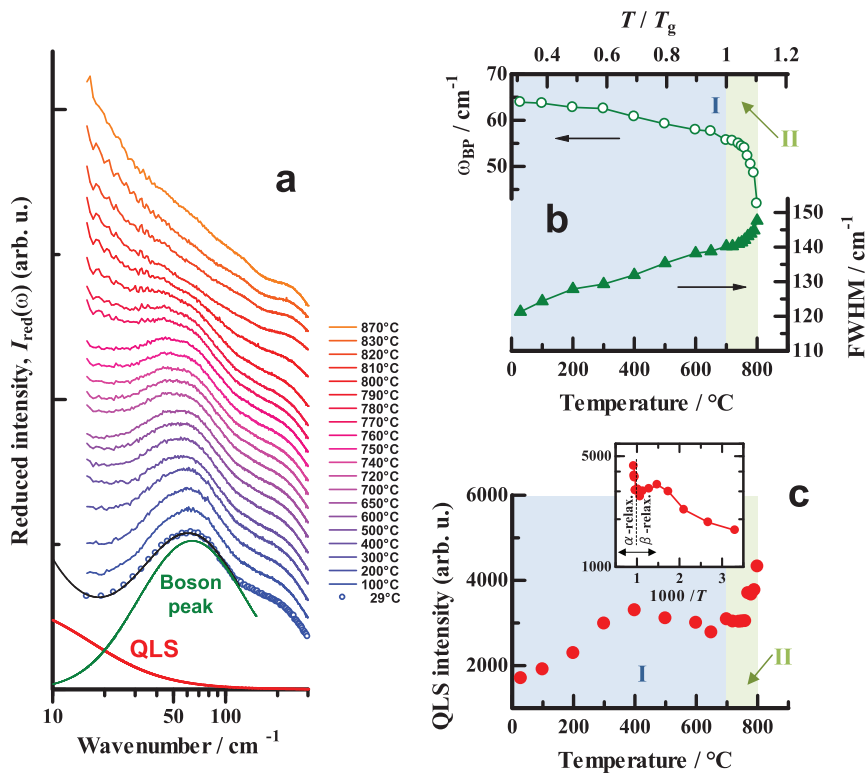


Figure 1 | In situ measurement of inelastic light scattering in the low-frequency region in the test glass with $0.67(2\text{BaO}-0.5\text{Na}_2\text{O})-1\text{P}_2\text{O}_5-2.5\text{Nb}_2\text{O}_5$ composition: (a) The reduced spectra during the heating process, (b) variation of the ω_{BP} and FWHM (circle and triangle, respectively) as a function of temperature and (c) QLS intensity as a function of temperature. In (a), the solid curve corresponds to the fitting result. The Boson peak and QLS components are also shown. The logarithmic QLS intensity as a function of inverse temperature is also provided as an inset for discussion (see text).

spectral intensity at which the frequency region is far below the Boson-peak frequency tended to increase during heating, i.e. QLS feature [Fig. 1(a)]. The intensity of the QLS component ($< \sim 40 \text{ cm}^{-1}$) increased and showed a maximum at 400°C , followed by a slight decrease in domain I. Subsequently, the intensity suddenly increased in domain II [Fig. 1(c)].

In situ observation of Raman scattering. Fig. 2 shows the observation results of the inelastic light-scattering spectra of the middle- and high-frequency regions, i.e. the Raman-scattering spectra. The spectrum at RT indicated two main bands with peaks at $\sim 800 \text{ cm}^{-1}$ and 650 cm^{-1} [Fig. 2(a)]. These bands may be assigned on the basis of the structure for niobate glasses in the study by Fukumi and Sakka¹⁰, i.e. the NbO_6 unit with non-bridging oxygen (NBO) and/or with much distortion: $\sim 800\text{--}900 \text{ cm}^{-1}$ and the less-distorted NbO_6 unit with no NBO: $\sim 600\text{--}800 \text{ cm}^{-1}$. To display the structural variation concerning the Nb–O polyhedral units during the heating process, the Raman spectra were tentatively deconvoluted into six Gaussian components (labelled ‘A’ to ‘F’). The sum of the band intensities contributed to the 800 cm^{-1} band (i.e. B and C) and the 650 cm^{-1} band (D and E), which were plotted as a function of temperature, in addition to a broad band at $\sim 1020 \text{ cm}^{-1}$ (A) due to the contribution of the symmetric stretching of phosphate Q^n units ($n = 0\text{--}2$; number of bridging oxygen) [Fig. 2(b)]¹¹. A remarkable change was observed in the intensities of the Nb-related bands, whereas no significant variation was observed in that of the 1020 cm^{-1} band: In domain I, the intensity of the 800 cm^{-1} band slightly increased, while that of the 650 cm^{-1} band slightly decreased. Subsequently, in domain II, an increase in the 800 cm^{-1} band intensity and a decrease in the 650 cm^{-1} band intensity were observed simultaneously (inset). By further increasing the temperature (domain III), a decrease and increase were observed in the intensities of the

800 cm^{-1} and 650 cm^{-1} bands, respectively. After the in situ observation, we observed numerous crystallites of approximately 5 nm dispersed in the test sample by field-emission transmission electron microscopy (FE-TEM).

Nanostructure evolution observation. Since an isothermal heating process, which was conducted at around the glass-transition temperature (T_g) for long treatment periods, promoted structural relaxation and the resulting ordering, a sequential snapshot during the relaxation and ordering processes was obtained by microscopic observation¹². Therefore, to understand how the nanostructuring proceeded during the in situ observation, FE-TEM and electron diffraction (ED) experiments were performed with the test sample being subjected to isothermal heat treatment. Fig. 3 shows the results of the FE-TEM observation of the test samples at the T_g ($= 695^\circ\text{C}$) for different treatment time periods. Although the non-treated sample did not show any structural change/ordering (sect. Method), prolonging the time resulted in nanometric-inhomogeneous regions with a few nm scale (5 h; a), which are attributed to the liquid–liquid phase separation; subsequently, numerous particles with sizes of $\sim 2\text{--}4 \text{ nm}$ (10 h; b) and $\sim 3\text{--}5 \text{ nm}$ (20 h; c) evolved. According to the corresponding ED patterns, although the 5-h sample exhibited only a halo pattern, the 10- and 20-h samples exhibited distinct ED rings, and a set of the ED rings could be identified with the NaNbO_3 (NN) phase [inset of Fig. 3(b)]. In addition, the ED-pattern-intensity profiles revealed the sequential nanostructure evolution in the supercooled liquid (SCL) phase [Fig. 3(d)]. Distinct peaks and a shoulder (dashed lines) also developed, which correspond to the nanostructured NN phase. For the 5-h sample, although the ED appeared to be a halo pattern, a small shoulder was noticed at the same position of the diffraction peak due to the (1 0 0) plane of the NN phase. Considering the corresponding FE-TEM image, it is strongly suggested

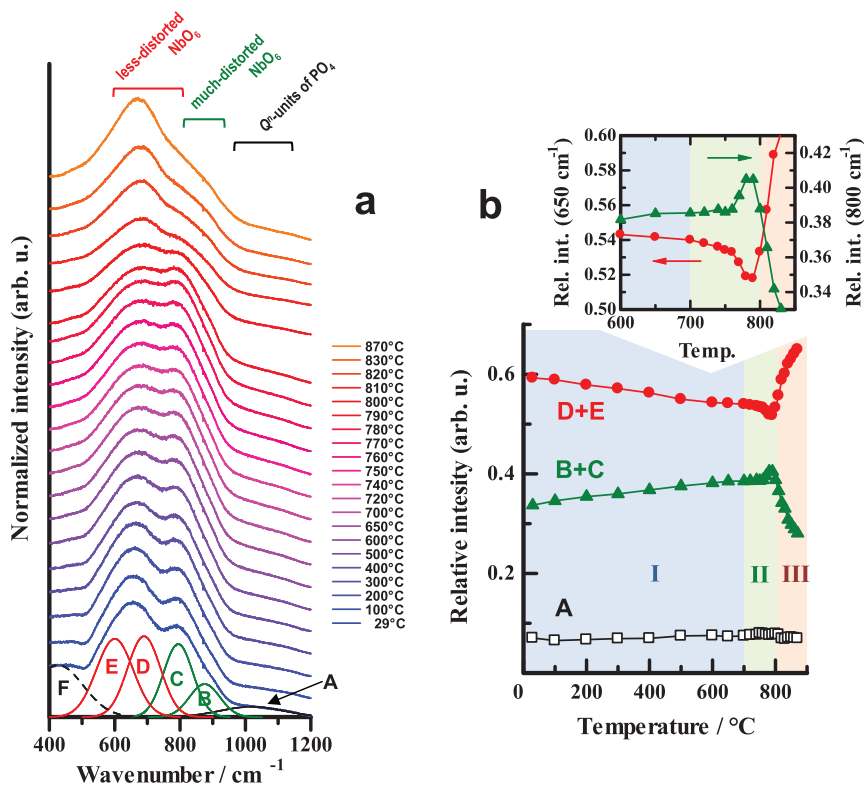


Figure 2 | In situ measurement of inelastic light scattering in the middle- and high-frequency regions, i.e. Raman scattering spectra, in the test glass: (a) The Raman spectra during the heating process, and (b) the variation of the relative intensities of the Raman bands concerning the Nb–O and phosphate units as a function of temperature. The obtained Raman spectra were normalized by the Bose–Einstein factor. In (b), an enlarged region of the intensities of 800 cm^{-1} and 650 cm^{-1} bands around the domain II is also indicated as an inset.

that the structural-ordering process occurs immediately after the nanometric phase separation.

Discussion

The QLS phenomenon in ferroelectrics and its relation to phase transitions have been studied, and the origin of QLS is attributed to the change in polarizability due to fluctuation, e.g. ion hopping and phase transition^{13–16}. According to Bouziane et al., the QLS in the antiferroelectric (AF) NN phase originates from the dipole relaxation around the off-centred octahedral NbO_6 units due to the AF phase transition, at which the off-centering displacement of Nb ions provides a zero average polarization¹⁴. In addition, Tsukada and Kojima studied the properties of a perovskite-type Nb relaxor by the broadband light scattering over the terahertz range (1 THz \approx 33 cm^{-1}) and observed that originates from the flipping/reorientation of octahedral units¹⁵. In terms of amorphous solids, it has been proposed that the QLS phenomenon is closely related to the fast β -relaxation process^{17–19}. Because 3D-interlinked NbO_6 units or the NbO_6 -nanodomain region has been verified in high- Nb_2O_5 -content glasses^{8,20,21}, the QLS studies of ferroelectrics would shed light on the QLS in glass. In other words, these studies help us to clarify the QLS in glass based on the analogy of the medium-range structure.

Prior to discussing the QLS features in the test sample, we consider the events that occurred in domains II and III. It may be possible to predict the events from the correlation between the variation of the 800 cm^{-1} /650 cm^{-1} band intensity and the nanostructure evolution in the isothermally treated samples: The samples subjected to isothermal treatment at the T_g undergo structural relaxation; thus, the Nb–O polyhedral units, which contributed to the network structure, are affected depending on the treatment period. Therefore, the band intensities express the degree of relaxation and provide information about the structural development during the in situ observation

using Fig. 2(b) as the calibration/standard curve. We measured Raman scattering spectra of the samples for the FE-TEM observation (5 h and 20 h) at RT. The measurement condition and analytic procedures were the same as in the case of the in situ observation. We obtained the following relative intensities from the results: $I_{\text{rel}}(800 \text{ cm}^{-1}) = 0.359$; $I_{\text{rel}}(650 \text{ cm}^{-1}) = 0.553$ for the 5-h sample and $I_{\text{rel}}(800 \text{ cm}^{-1}) = 0.321$; $I_{\text{rel}}(650 \text{ cm}^{-1}) = 0.593$ for the 20-h sample. These values show that the isothermally treated 5- and 20-h samples correspond to the samples observed in situ at $\sim 810^\circ\text{C}$ and $\sim 830^\circ\text{C}$, respectively. By considering the abovementioned FE-TEM results, domains II and III can correspond to the ‘nanometric phase separation’ and ‘nanocrystallization’ regimes, respectively. The conclusion is reasonable because domain II is the temperature region above the T_g , and a rapid decrease of the Boson-peak frequency was observed, indicating elastic softening due to the glass–SCL transition or α -relaxation⁷. If the relaxation decreases, the constituent atoms acquire sufficient fluidity to migrate/diffuse in the SCL phase, leading to phase separation and structural ordering. In a previous study concerning the relation between the Boson-peak behaviour and phase separation, a small damping of the Boson peak was confirmed during the heating process and was attributed to phase separation²². Therefore, the broadening of the Boson peak in domain II [Fig. 1(b)] also supports the nanometric phase separation. With regards to domain III, the increase in the 650 cm^{-1} band (the less-distorted NbO_6 unit with no NBO) was observed. Because the structure related to the 650 cm^{-1} band is regarded to be the interlinked- NbO_6 units that resemble a perovskite-type 3D structure, by considering the FE-TEM and ED results, the development of the 650 cm^{-1} band probably originate from the grown NN nanocrystals.

Here we begin to discuss the origin of QLS. For domain II, the NbO_6 units consisting of the network structure undergo a drastic structural change due to the phase separation via α -relaxation. In

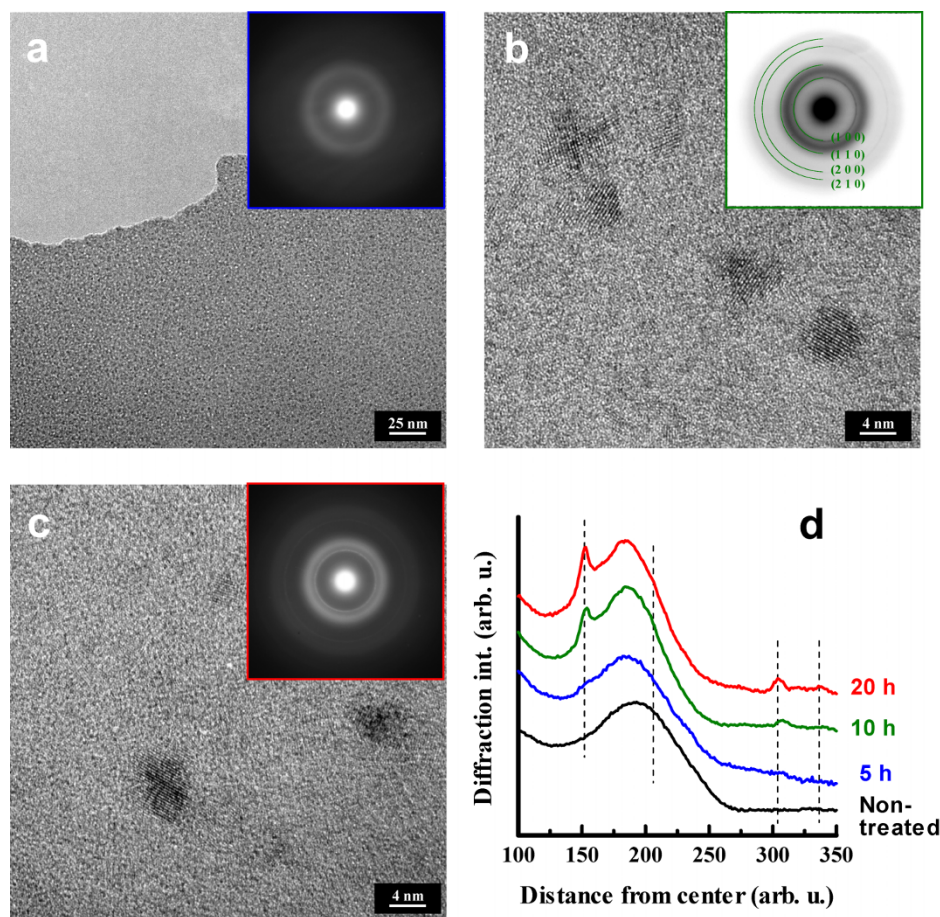


Figure 3 | Morphological and phase-formation analyses in isothermally heat-treated samples: FE-TEM images and corresponding selected-area ED patterns of the test sample subjected to isothermal heat-treatment at 695 °C for 5 h (a), 10 h (b) and 20 h (c). Their ED intensity profiles are also included in addition to that of the non-treated sample (d). In (b), the semicircles were drawn on the basis of crystallographic data of perovskite-type NaNbO_3 (ICDD: 75-2102). In (d), the peaks/shoulder and a broad peak are due to the perovskite-type NN and first halo peak of the glassy phase, respectively.

particular, we noticed the increase of the 800 cm^{-1} band. Assuming that the much-distorted NbO_6 unit (800 cm^{-1} band) is comparable with the off-centred NbO_6 octahedron, the increase is attributed to the transformation of the less-distorted octahedral unit to the off-centred unit. Taking the abovementioned descriptions [Bouziane et al. (Ref. 14)], we can interpret the QLS in domain II as a momentary change of the Nb displacement in the off-centred NbO_6 units, which provide polarization fluctuations, by the nanometric phase separation in the α -relaxation regime. In a previous study, the in situ inelastic light scattering in niobiogermanate glass revealed a drastic rearrangement of the network structure during the elastic-softening period, and the crystal nuclei evolve in the period owing to structural ordering in the nanometrically inhomogeneous region^{7,8}. Because this situation is almost the same as that in this study, we realize that domain II corresponds to the ‘nanocrystallization precursive stage’. Thus, it was demonstrated that the QLS phenomenon is caused by phase separation/nucleation in the precursive stage. In other words, the QLS originates in a ‘large structural disturbance’. Furthermore, we need to consider the QLS phenomenon in domain III, in which the Boson peak vanished [Fig. 1(a)]. Because the NN nanocrystals grow and mature in this domain, we considered that the nanocrystals largely govern the spectral/QLS feature in domain III in accordance Bouziane’s study¹⁴. In other words, the SCL phase governs the QLS in domain II, whereas the predominance of the QLS has already been shifted to the NN nanocrystals above 800°C , i.e. domain III.

Although we observed a gentle increase in the QLS intensity and its maximum around 400°C [Fig. 1(c)], these could not be explained

by the above discussion because negligible contribution is expected from α -relaxation in domain II, which is far below the T_g , at which β -relaxation is dominant. Therefore, it is necessary for it to be considered from another aspect: The QLS phenomenon has been also identified in ion-conducting crystals as well as the ferroelectrics^{23,24}. According to Suemoto and Ishigame¹³, QLS is caused by the polarization fluctuation due to ion hopping, and the temperature dependence of the QLS intensity, $S(\omega)$, is expressed by

$$S(\omega) \propto \alpha^2 \frac{[\Gamma_0 \exp(-\Delta/kT)]}{[(\Gamma_0 \exp(-\Delta/kT))^2 + \omega^2]}, \quad (1)$$

where α is the polarizability and ω is the frequency. The component in square brackets corresponds to a non-zero eigenvalue that represents the hopping rate. Because the component has an activation-type dependence on the temperature (Δ : activation energy; Γ_0 : pre-exponential factor), the $\log(S) - 1/T$ plot ideally shows a convex curve (This was experimentally verified in the ion-conducting crystals, e.g. yttrium-stabilized zirconia, Na-doped alumina, etc.)^{13,23,24}. Because the frequency region of the ion-conducting crystals is within ~ 0.1 – 1 cm^{-1} (i.e. the Brillouin region), which is much lesser than the frequency region in our study (low-frequency Raman), it appears to be difficult to directly apply this theory to the observed QLS intensity in domain I for quantitative analysis. However, the Nb_2O_5 – P_2O_5 glass system possesses a relatively high ionic conduction^{25–27}; thus, it appears to be reasonable to use the theory for qualitative discussion. Because the QLS feature of domain I is very similar



to that of the conducting crystals, i.e. the convex curve [inset of Fig. 1(c)], we can propose a possible scenario for the variation intensity as follows: in the glassy state around RT, a conductible ion, Na^+ , exists in the vicinity of the NbO_6 unit for charge compensation. During the heating process, the migration (or hopping) of the conducting ions causes a momentary change in the displacement of Nb, which may be smaller than the displacement in domain II (or the α -relaxation regime). Consequently, the small polarization fluctuation is responsible for the QLS in domain I (or the β -relaxation regime). Several authors have reported that below the T_g , the QLS phenomenon in the glassy/SCL phase is attributed to β -relaxation^{17–19}. In this study, the origin of the QLS observed in domain I can be interpreted as the fluctuation due to Na migration; that is, a ‘small structural disturbance’.

In summary, QLS variations were observed in two temperature domains and their origins were expressed relatively concretely, i.e. the polarization fluctuation caused by the structural disturbance concerning the NbO_6 unit (SCL phase; α -relaxation regime) and that caused by the motion of conducting ions localized in the vicinity of the NbO_6 unit (below the T_g ; β -relaxation regime). Furthermore, this study gives the possible evidence for the presence of a nanometric cohesive region in the glassy state, i.e. the NbO_6 -polyhedral cluster, which is capable of reorientation/displacement. It also corroborated the nanocrystallization of niobate phases^{5,9,28} and the high optical nonlinearity in the Nb_2O_5 -containing multicomponent glasses^{29,30}. Although further studies are necessary to clarify the QLS phenomenon, we hope that this study will provide a better understanding of the relaxant and crystallization in oxide glass.

Methods

Test sample preparation. The test sample employed in this study was phosphoniobate glass, in which Nb ferroelectrics are nanostructured, i.e. $0.67(2\text{BaO}-0.5\text{Na}_2\text{O})-1\text{P}_2\text{O}_5-2.5\text{Nb}_2\text{O}_5$ glass⁹. Because the resulting nano GC exhibits excellent optical transmittance similar to that exhibited by the glass precursor, the sample is suitable for spectroscopic studies based on the light-scattering phenomenon. The glass was synthesized using a conventional melt-quenching technique (The detailed procedure is described in Ref. 9). The obtained as-quenched glass was annealed at the T_g for 1 h to reduce the internal stress. No crystallization could be confirmed in the glass using FE-TEM and ED analysis, i.e. the completely amorphous phase. Therefore, this glass was employed as the test sample. For thermal and morphological analyses, differential thermal analysis (DTA) and X-ray diffraction (Cu-K α) were utilized in addition to FE-TEM and ED.

Spectroscopic observation. Inelastic light-scattering spectra (Stokes side) in the low-frequency (i.e. QLS and Boson peak) and middle–high-frequency (Raman) regions of the test glass were measured using an Ar⁺-gas laser operating at 514.5 nm and a system consisting of a triple-grating monochromator and liquid-nitrogen-cooled charge-coupled device detector (HORIBA-Jobin Yvon, T64000). The spectral measurement was performed while elevating the temperature from room temperature (RT) using a temperature-controlling system (Linkam Scientific Instruments). In the low-frequency region, the obtained spectra were reduced with respect to the Bose–Einstein factor, producing the reduced intensity, $I_{\text{red}}(\omega)$, as described by Shuker and Gammon³¹:

$$I_{\text{red}}(\omega) = \frac{I_{\text{obs}}(\omega)}{\omega[n(\omega, T) + 1]} \propto \frac{C(\omega)g(\omega)}{\omega^2}, \quad (2)$$

where $I_{\text{obs}}(\omega)$ is the observed intensity of the spectra, $n(\omega, T)$ is the Bose–Einstein factor, $C(\omega)$ is the light-vibration-coupling factor and $g(\omega)$ is the vibrational density of the states. To evaluate the QLS and Boson-peak contributions in the low-frequency region, the reduced spectra were fitted using the sum of two Lorentzian functions (the maximum peak are centred at 0 cm^{-1}) and a log-normal function, which correspond to Rayleigh, QLS and Boson-peak components, respectively.

- Rosenflanz, A. *et al.* Bulk glasses and ultrahard nanoceramics based on alumina and rare-earth oxides. *Nature* **430**, 761–764 (1999).
- Martinez, L.-M. & Angell, C. A. A thermodynamic connection to the fragility of glass-forming liquid. *Nature* **410**, 663–667 (2001).
- Sakamoto, A. & Yamamoto, S. Glass-ceramics: Engineering principle and applications. *Int. J. Appl. Glass Sci.* **1**, 237–247 (2010).
- Orava, J., Greer, A. L., Gholipour, B., Hewak, D. W. & Smith, C. E. Characterization of supercooled liquid $\text{Ge}_2\text{Sb}_2\text{Te}_5$ and its crystallization by ultrafast-heating calorimetry. *Nat. Mater.* **11**, 279–283 (2012).

- Falcão-Filho, E. L. *et al.* Third-order optical nonlinearity of a transparent glass ceramic containing sodium niobate nanocrystals. *Phys. Rev. B* **69**, 134204–134212 (2004).
- Zhou, Y., Zhang, Q., Luo, J., Tang, Q. & Du, J. Structural and dielectric characterization of Gd_2O_3 -added $\text{BaO}-\text{Na}_2\text{O}-\text{Nb}_2\text{O}_5-\text{SiO}_2$ glass-ceramic composites. *Scripta Mater.* **65**, 296–299 (2011).
- Takahashi, Y., Osada, M., Masai, H. & Fujiwara, T. Crystallization and nanometric heterogeneity in glass: In situ observation of the boson peak during crystallization. *Phys. Rev. B* **79**, 214204–214209 (2009).
- Takahashi, Y., Masai, H., Osada, M. & Fujiwara, T. Precursive stage of nanocrystallization in niobium oxide-containing glass. *Appl. Phys. Lett.* **95**, 071909–071912 (2009).
- Takahashi, Y., Fujie, N. & Fujiwara, T. Nano-sized $\text{Ba}_2\text{NaNb}_3\text{O}_{15}-\text{NaNbO}_3$ co-crystallized glass-ceramics in phosphoniobate system. *Appl. Phys. Lett.* **100**, 201907–201911 (2012).
- Fukumi, K. & Sakka, S. Coordination state of Nb^{5+} ions in silicate and gallate glasses as studied by Raman spectroscopy. *J. Mater. Sci.* **23**, 2819–2823 (1988).
- Mazali, I. O., Barbosa, L. C. & Alves, O. L. Preparation and characterization of new niobophosphate glasses in the $\text{Li}_2\text{O}-\text{Nb}_2\text{O}_5-\text{CaO}-\text{P}_2\text{O}_5$ system. *J. Mater. Sci.* **39**, 1987–1995 (2004).
- Takahashi, Y., Ando, M., Ihara, R. & Fujiwara, T. Formation of Zn defects in willemite-type Zn_2GeO_4 during supercooled liquid-crystal phase transition. *Appl. Phys. Lett.* **98**, 221907–221910 (2011).
- Suemoto, T. & Ishigame, M. Determination of the ionic diffusion constant by using a quasi-elastic light scattering. *Solid State Ionics* **9** & **10**, 1365–1370 (1983).
- Bouziane, E., Fontana, M. D. & Ayadi, M. Study of the low-frequency Raman scattering in NaNbO_3 crystal. *J. Phys.: Condens. Matter* **15**, 1387–1395 (2003).
- Tsukada, S. & Kojima, S. Broadband light scattering of two relaxation processes in relaxor ferroelectric $0.93\text{Pb}(\text{Zn}_{1/3}\text{Nb}_{2/3})\text{O}_3-0.07\text{PbTiO}_3$ single crystals. *Phys. Rev. B* **78**, 144106–144112 (2008).
- Sivasubramanian, V. & Kojima, S. Brillouin scattering studies of acoustic phonon modes and central peak in single-crystal $\text{Pb}(\text{Sc}_{1/2}\text{Ta}_{1/2})\text{O}_3$. *Phys. Rev. B* **85**, 054104–054110 (2012).
- Kanaya, T., Kawaguchi, T. & Kaji, K. Low energy excitation and fast motion near T_g in amorphous cis-1,4-polybutadiene. *J. Chem. Phys.* **98**, 8262–8270 (1993).
- Brodin, A., Börjesson, L., Engberg, D., Torell, L. M. & Sokolov, A. P. Relaxational and vibrational dynamics in the glass-transition range of a strong former B_2O_3 . *Phys. Rev. B* **53**, 11511–11520 (1996).
- Ribeiro, M. C. C. Low-frequency Raman spectra and fragility of imidazolium ionic liquid. *J. Chem. Phys.* **133**, 024503–024509 (2010).
- Cardinal, T. *et al.* Erbium luminescence properties of niobium-rich oxide glasses. *J. Non-Cryst. Solids* **351**, 2076–2084 (2005).
- Royon, A. *et al.* Strong nuclear contribution to the optical Kerr effect in niobium oxide containing glasses. *Phys. Rev. B* **75**, 104207–104213 (2007).
- Takahashi, Y., Osada, M., Ando, M., Ihara, R. & Fujiwara, T. Low-frequency inelastic light scattering of zincogermanate glass in supercooled liquid regime. *J. Appl. Phys.* **109**, 126105–126105–3 (2011).
- Suemoto, T. & Ishigame, M. Quasielastic light scattering in superionic β -alumina. *Phys. Rev. B* **32**, 4126–4133 (1985).
- Suemoto, T. & Ishigame, M. Quasielastic light scattering in oxygen-ion conductors. *Phys. Rev. B* **33**, 2757–2764 (1986).
- Barth, St. & Feltz, A. Structure and ionic conduction in solid. VII. Ion conducting glasses in the system $\text{Na}_2\text{O}-\text{Nb}_2\text{O}_5-\text{P}_2\text{O}_5$. *J. Non-Cryst. Solids* **34**, 41–45 (1989).
- Chowdari, B. V. R. & Radhakrishnan, K. Preparation and characterization of rf-sputtered thin films of $\text{Li}_2\text{O}-\text{P}_2\text{O}_5-\text{Nb}_2\text{O}_5$ glasses. *Solid State Ionics* **44**, 325–329 (1991).
- Okada, T., Honma, T. & Komatsu, T. Synthesis and Li^+ ion conductivity of $\text{Li}_2\text{O}-\text{Nb}_2\text{O}_5-\text{P}_2\text{O}_5$ glasses and glass-ceramics. *Mater. Res. Bull.* **45**, 1443–1448 (2010).
- Venkataraman, B. H. & Varma, K. B. R. Nanocrystallization of ferroelectric strontium bismuth vanadium niobate in lithium tetraborate glasses. *J. Nanosci. Nanotechnol.* **5**, 2108–2116 (2005).
- Vogel, E. M. *et al.* Structural and optical study of silicate glasses for nonlinear optical devices. *J. Non-Cryst. Solids* **107**, 244–250 (1989).
- Dassauze, M. *et al.* Correlation of large SHG responses with structural characterization in borophosphate niobium glasses. *Opt. Mater.* **28**, 1417–1422 (2006).
- Shuker, R. & Gammon, R. W. Raman-scattering selection-rule breaking and the density of states in amorphous materials. *Phys. Rev. Lett.* **25**, 222–225 (1970).

Acknowledgements

This work was supported by the Ministry of Education, Culture, Sports, Science and Technology of the Japanese Government. The authors would like to thank Mr. Nobuhiro Fujie of the Department of Applied Physics, Graduate School of Engineering, Tohoku University, for providing the test sample. Dr. Takamichi Miyazaki of the Department of Instrumental Analysis, School of Engineering, Tohoku University and Dr. Kiyotaka Iijima of the International Center for Materials Nanoarchitectonics, National Institute for Materials Science significantly contributed to this study.



Author Contributions

Y. T. and T. F. designed the study. Y. T. and K. N. performed experiments to characterize the test sample, and K. N. and M. O. performed the spectroscopic observation. Y. T. and T. F. wrote the paper.

Additional information

Competing financial interests: The authors declare no competing financial interests.

License: This work is licensed under a Creative Commons Attribution-NonCommercial-ShareAlike 3.0 Unported License. To view a copy of this license, visit <http://creativecommons.org/licenses/by-nc-sa/3.0/>

How to cite this article: Takahashi, Y., Nakamura, K., Osada, M. & Fujiwara, T. Structural relaxation and quasi-elastic light scattering in glass: Approach by ferroelectric and ion-conducting phases. *Sci. Rep.* 2, 714; DOI:10.1038/srep00714 (2012).